ACS APPLIED BIO MATERIALS

www.acsabm.org Article

Harnessing Fe(III)−Carboxylate Photochemistry for Radical-Initiated Polymerization in Hydrogels

M. H. Jayan S. Karunarathna, Abigail N. Linhart, Giuseppe E. Giammanco, Amie E. Norton, Jackson J. Chory, Jason J. Keleher,* and Alexis D. Ostrowski*

Cite This: *ACS Appl. Bio Mater.* 2021, 4, 5765−5775 Read Online

ACCESS | Metrics & More | Article Recommendations | Supporting Information

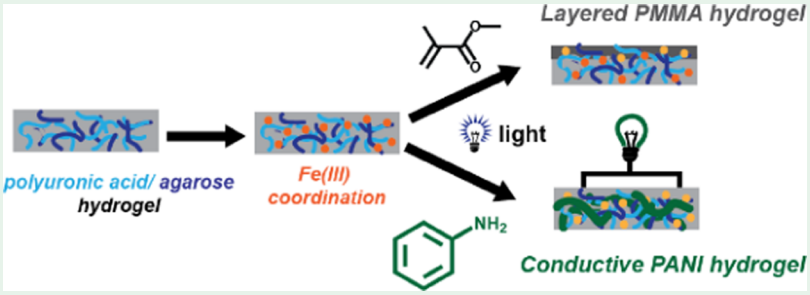

ABSTRACT: Coordination of Fe(III) to carboxylates in polyuronic acid hydrogels was used to impart photochemical reactivity to polysaccharide-based hydrogels. This photochemical reaction was then used for light-initiated polymerization to create hydrogels with advanced mechanical and conductive properties by capturing the photogenerated radical with a monomer, either acrylamide, methyl methacrylate, or aniline. The photopolymerization of acrylamide using the Fe(III)−polyuronic acid was quantified in solution and the polymerization efficiency was determined under different conditions. Poly(methyl methacrylate) (PMMA)-modified hydrogels were analyzed by the contact angle, optical microscopy, and rheology. This confirmed formation of a stiff, hydrophobic, PMMA layer on polysaccharide hydrogels after light irradiation in methyl methacrylate. Polyaniline-modified hydrogels were characterized by current−voltage sweeps, which showed the formation of conductive polyaniline integrated into the hydrogel after light irradiation in the aniline monomer. This strategy provided a facile approach to create either layered hydrogels with different stiffness and hydrophobicity or hybrid conductive hydrogels using the simple photochemical reaction of blue light irradiation of Fe(III) coordinated to polyuronic acids.

KEYWORDS: *photopolymerization, conductive hydrogels, Fe(III) photochemistry, radical polymerization, hydrogel modification*

INTRODUCTION

From contact lenses to gelatin desserts, hydrogels show up in a variety of applications, even in daily life. The porous nature and softness of hydrogels can mimic natural living tissues, so hydrogels are widely used in biomedical applications, including hygiene products, scaffolds for tissue engineering, drug delivery systems, and wound dressings.[1,2] Postsynthetic surface modification of hydrogels can be used to tune the chemical and mechanical properties of materials to create advanced materials such as superhydrophobic surfaces, adhesives, and antifouling coatings.[3,4] Conductive hydrogels can also be designed for applications in wearable and implantable devices, biosensors, health recording electrodes, and medical patches.[5] Polyaniline (PANI) has emerged as one of the most commonly used polymers to give conductivity to hydrogels due to its high conductivity, ease of synthesis, and pH-dependent properties.[6−11] However, due to the large amount of water in hydrogels, postsynthetic modification of many of these materials remains a challenge, especially using biofriendly reagents.

Photoinitiated radical polymerization has emerged as a facile method for postsynthetic modification of materials since the time, area, and amount of modification can be easily controlled by changing the irradiation time, area, and light intensity.[12] A variety of photoinitiators have been used to initiate polymerization in hydrogels, but for this work, we focused on using an earth-abundant, bioinspired photoinitiator based on Fe(III) complexes. Iron-based photoinitiators have been used successfully to create hybrid hydrogel materials.[13−15] Typically, these photoinitiators are specially designed iron−amine complexes. However, this work looks to use more bioavailable, lower-cost alternatives, iron−carboxylate complexes.

Received: May 6, 2021
Accepted: June 10, 2021
Published: June 24, 2021

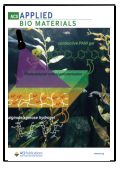

The photochemistry of Fe(III)−carboxylates is known to occur in a variety of natural systems.[16−18] In particular, previous work has explored the photochemistry of Fe(III)−carboxylate-containing polysaccharides (polyuronic acids) which occurs via a radical process (Figure 1).[19] Upon exposure

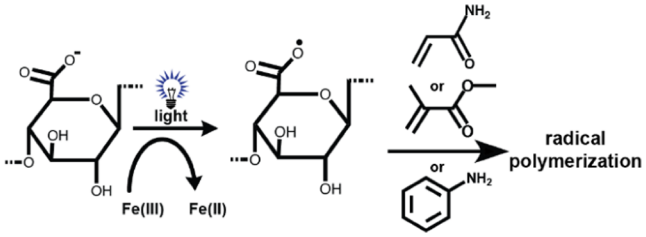

Figure 1. Scheme for photoinitiated radical polymerization using Fe(III) polyuronates.

to 405 nm or shorter wavelength light, electron transfer from carboxylate to Fe(III) generates a radical on the polymer chain or free carbon dioxide anion radicals in solution.[20] Both Fe(III) and polyuronic acids are earth abundant, inexpensive, and biocompatible. They also show efficient photoreactivity (QY ∼ 0.1) in aerated aqueous environments, ideal to use for photoinitiated processes in hydrogel materials.

This work utilizes the coordination of Fe(III) to polyuruonic acids for photoinitiation of radical polymerization of acrylates and aniline in these naturally derived hydrogel materials. Through this photoinitiation process, postsynthetic modification of polysaccharide hydrogels creates mechanically robust layered or conductive hydrogel materials, depending on the type of monomer used in the radical polymerization process. We focus here on polymerization of acrylates to create layered hydrogel/poly(methyl methacrylate) (PMMA) materials and polymerization of aniline to form conductive polyaniline (PANI) hydrogels.

RESULTS AND DISCUSSION

Fe(III)−Polysaccharide Photochemistry in Hydrogels. Previous work has shown that the Fe(III)−polyuronate photochemistry can not only take place in polysaccharide solutions but also in hydrogel systems with alginate, pectate, and hyaluronate mixed with acrylamide.[19,21] This work shows that polysaccharide hydrogel materials can be prepared using these different polysaccharides mixed with agarose, and that the Fe(III)−polyuronic acid photochemistry can be utilized to change hydrogel properties. These materials showed significant changes in chemical and physical properties upon the introduction of Fe(III) and light irradiation. Young's modulus of Fe(III) pectin/agarose hydrogels changed with the irradiation time, compared to control pectin/agarose gels with no Fe(III) showing the role of Fe(III) in this photoreaction (Figure S1).[21] This decrease of modulus upon light irradiation in Fe(III) pectin/agarose gels is due to the photoreaction of Fe(III)−pectin and subsequent degradation of the pectin polymer chain. Furthermore, a decrease in swelling ratio upon irradiation was seen due to the decarboxylation process (Figure S2). This process reduced the number of hydrophilic sites within the matrix, thereby decreasing the amount of water that can be effectively held in the gel. To further validate the decarboxylation mechanism, Congo red solution was used as an indicator to visualize the photoreaction via pH changes (Figure S3). Fe(III) pectin/agarose hydrogels stored in dark were blue (pH < 3), while a red (pH > 5) color was observed for irradiated gel samples (Figure S3c). The blue color indicates acidic carboxylate groups and Fe(III) in the gels stored in dark, whereas the irradiated hydrogels retained the red color due to the higher pH from the decarboxylation and Fe(II) formation.

Harnessing the Radical for Surface Modification of Pectin/Agarose Hydrogel Materials. To harness this photochemistry for postsynthetic modification of hydrogels, capturing the generated radical (Figure 1) to initiate

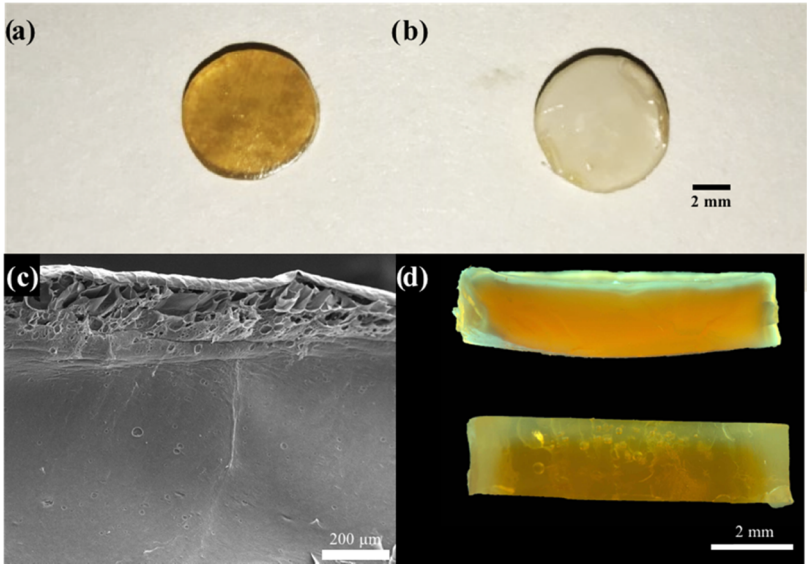

Figure 2. (a) Photo of the Fe(III) pectin/agarose hydrogel disk placed in MMA for 2 h in dark. (b) Photo of the Fe(III) pectin/agarose hydrogel disk placed in MMA and irradiated with 405 nm light-emitting diode (LED) (50 mW cm^{-2}) for 2 h. (c) Scanning electron microscopy (SEM) image of the Fe(III) pectin/agarose hydrogel surface modified with 25% MMA solution using 405 nm LED (50 mW cm^{-2}) for 2 h. (d) Light microscope image of two Fe(III) pectin/agarose hydrogel cross sections, the top irradiated with 405 nm LED (50 mW^{-2}) in 25% MMA for 2 h and bottom-placed in 25% MMA and stored in dark for 2 h.

https://doi.org/10.1021/acsabm.1c00525
ACS Appl. Bio Mater. 2021, 4, 5765−5775

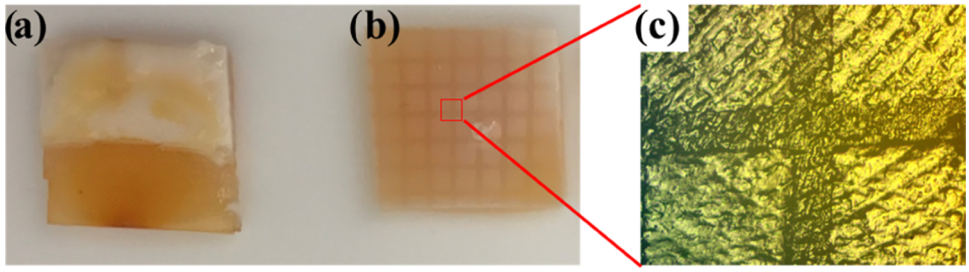

Figure 3. (a) Photo of the Fe(III) pectin/agarose hydrogel with top half surface modified with PMMA using a photomask to block the bottom of the gel from light (50 mW cm^{-2}, irradiated for 2 h), (b) Photo of the Fe(III) pectin/agarose hydrogel surface modified with PMMA in a grid pattern by placing a wire mesh on top of the gel during irradiation (50 mW cm^{-2}, irradiated for 2 h), and (c) optical microscope image of the grid pattern in (b) with 10× magnification.

polymerization reactions on the surface or within the matrix of the hydrogel is imperative. For these studies, methyl methacrylate (MMA) was chosen due to the differences in hydrophobicity to tune the physical properties of hydrogel materials. When Fe(III) pectin/agarose hydrogels were irradiated (405 nm, 50 mW cm^{-2}) in solutions of MMA, the gels showed significant changes in their chemical and physical properties. The Fe(III) pectin/agarose hydrogels irradiated in MMA showed a white color on the surface (Figure 2b), indicating that poly(methyl methacrylate) (PMMA) was generated on top of the hydrogel disk during irradiation. In dark conditions, MMA polymerization was not observed (Figure 2a).

The PMMA-modified Fe(III) pectin/agarose hydrogels were characterized by SEM (Figure 2c) and optical microscopy (Figure 2d). The SEM imaging of the surface-modified pectin−agarose gel cross section (Figure 2c) showed the PMMA layer on the top of the gel. This nonporous PMMA layer on top of the porous 2 mm thick gel disk is evident in the SEM images (Figure 2c) and was measured to be 35 ± 5 μm thick. When PMMA surface-modified gel disk cross sections were observed under the light microscope, clear differences were seen compared to the gel from dark control (Figure 2d). Gels stored in the dark were more transparent, whereas the samples exposed to the 405 nm LED were more translucent due to the PMMA polymerization.

The role of light was confirmed by creating patterns and controlling the area of PMMA polymerization using photomasks. Only the area exposed to light showed white solid MMA polymerization (Figure 3a). Building on this result, a small wire mesh was used as a photomask. This created a grid pattern on the hydrogel (Figure 3b). This pattern was clearly visible under an optical microscope (Figure 3c) and was accompanied by hydrophilic/hydrophobic regimes. Specifically, the areas modified with PMMA would be more hydrophobic, while the hydrogels Fe(III) pectin/agarose would be more hydrophilic. This shows that the gels' surface hydrophobicity/hydrophilicity can be patterned via photocontrolled surface modification.

To further characterize the parameters for effective photopolymerization, the effects of O_2 on PMMA polymerization in hydrogels were also studied. When the irradiation of Fe(III) pectin/agarose gels was performed under N_2, the polymerization on the gels was significant after 15 min of irradiation compared to the irradiation in air (Figure S4). This indicated that the polymerization was occurring due to the radical formed during the photoreaction and the previously observed lower efficiency of photoreaction due to oxygen slowed down the polymerization. The oxygen inhibition of radical polymerization processes is well known, and there is a growing interest in developing oxygen tolerant radical polymerization processes.[22]

Solution Studies of Radical Initiation with the Fe(III)−Polyuronic Acid. Based on these results with pectin, the Fe(III)−carboxylate photochemistry was expanded to that of another polysaccharide, alginate. Alginate is a polymer of interest due to its hydrophilicity and greater number of carboxylates per unit (i.e., four per unit in alginate and one per unit in pectin).

Due to its aqueous solubility, the monomer acrylamide (AAM) was used to study the kinetics of radical polymerization in solution using Fe(III) alginate (Fe(III) AlgM) as a soluble model reaction. The polymerization of monomer (M) in the presence of a given Fe(III)−L complex as a photoinitiator of radicals can be described by the following eqs 1−5

Initiation:

$$\mathrm{Fe(III)L} \xrightarrow{h\nu} \mathrm{Fe(II)} + \mathrm{L}^{*}\ R_i = k_i[\mathrm{Fe(III)L}] \tag{1}$$

Propagation:

$$\mathrm{L}^{*} + \mathrm{M} \rightarrow \mathrm{L-M}^{*} \xrightarrow{\mathrm{M}} \mathrm{P}^{*} \quad R_\mathrm{p} = k_\mathrm{p}[\mathrm{L}^{*}][\mathrm{M}] \tag{2}$$

Termination:

$$P^{*} + P^{*} \rightarrow \text{polymer} \quad R_\mathrm{t} = k_\mathrm{t}[P^{*}]^2 \tag{3}$$

$$P^{*} \rightarrow \text{polymer}\ R_\mathrm{t} = k'_\mathrm{t}[P^{*}] \tag{4}$$

$$P^{*} + \mathrm{L}^{*} \rightarrow \text{polymer} \quad R_\mathrm{t} = k''_\mathrm{t}[\mathrm{L}^{*}][\mathrm{P}^{*}] \tag{5}$$

where L is alginate or other polyuronic acid ligand (e.g., pectin). Assuming the steady-state approximation, the rate of polymerization (R_p) can be derived in eq 6

$$R_\mathrm{p} = \frac{k_\mathrm{p}}{k_\mathrm{t}}[I_\mathrm{a}\Phi_i]^{1/2}[\mathrm{M}] \tag{6}$$

where the rate constants for polymerization and radical formation are k_p and k_t, Φ_I is the quantum yield of radical formation, [M] is the concentration of the monomer, and I_a is the absorbed light intensity (units = Einsteins = moles of photons).

To study the kinetics of the formation of polysaccharide radicals, we assumed that the reduction of each Fe(III) ion yields a single radical. Thus, by quantifying the Fe(II) photoproduced, we calculated the rate of initiation, and thus, the initiation quantum yield:

https://doi.org/10.1021/acsabm.1c00525
ACS Appl. Bio Mater. 2021, 4, 5765−5775

$$\Phi_I = \Phi_{\mathrm{Fe(II)}} = \frac{R_f}{I_a} \quad (7)$$

$$\phi_{\mathrm{Fe(II)}} = \frac{n\mathrm{Fe(II)}}{I_0(1 - 10^{-\mathrm{Abs}})} \quad (8)$$

where R_f is the moles of polysaccharide radicals, nFe(II) is the moles of ferrous iron produced during the photoreaction, I_0 is the incident moles of photons (as determined by ferrioxalate actinometry[23]), and Abs is the absorbance of the sample at the irradiation wavelength (405 nm).

As shown in Figure S5, the rate of formation of Fe(II) was independent of the concentration of the AAM monomer; in fact, it was not affected by the presence of acrylamide at all. On the other hand, the presence of oxygen did have an effect on $\Phi_{\mathrm{Fe(II)}}$, just as observed in previous work.[19]

When a Fe(III) AlgM photointiator complex was irradiated in the presence of the reactive monomer acrylamide (AAM), the absorbance of the solution decreased upon irradiation, agreeing with the reduction of Fe(III) (Figure S6a,b). The amount of reacted monomer was determined from the integration of the ^{1}H NMR spectrum (Figure S6c), and this information was used to calculate the polymerization quantum yield, Φ_P, defined as the moles of reacted monomer per mol of photons (Einsteins) (Figures S7a and S6d).

If the reaction follows the described kinetics for polymerization (eq 6), then it should be first order with respect to [AAM] and 1/2 order with respect to the intensity of the light. Although many radical polymerizations present a first-order dependence of the polymerization rate with the monomer concentration, (eq 6) our results indicated a nonlinear relationship of the polymerization quantum yield with [AAM] (Figure S7a,b). Such behavior could be indicative of a change in the efficiency of the initiation process due to the presence of the monomer.[24] In our particular case, an order of n = 7 with respect to [AAM] (Figure S7c) suggests that the rate-limiting step of the reaction was not the formation of the radical initiator (eq 1), but the reaction of that radical with the first molecule of the monomer in the very primary stage of the propagation (eq 2), a common behavior for light-initiated agents.[24] Furthermore, the rate of the reaction decreased as the reaction mixture was diluted, for a fixed AAM to Fe(III)−AlgM ratio (Figure S7d). The kinetic chain length was calculated:

$$\mathrm{kcl} = \frac{R_p}{R_i} \quad (9)$$

where R_p was the rate of polymerization determined from eq 6 and R_i was the rate of initiation calculated from eq 7. Using 0.56 M AAM solution, the calculated kinetic chain length (kcl) (eq 9) was 500. This means that, on average, 500 AAM monomer units were added to a single chain initiated by a single radical in the conditions of this experiment.

It must also be noted, when using pectate as the uronate-containing ligand, the product of the photochemical reaction could be purified and analyzed by ^{1}H NMR. Figure S8 shows the spectra of the photopolymerized polyacrylamide obtained upon irradiation of Fe(III)/AAM (control) for 1 h, and Fe(III)−pectate/AAM for 15 min. By rinsing the copolymeric product with hot morpholine (polyacrylamide soluble, polysaccharide insoluble), we could confirm that the polymer product was a graft copolymer and not a mixture of homopolymers. These results highlight that Fe(III)−uronic acids can be used for effective photoinitiation in solution to produce grafted polymers on the polysaccharide ligand.

Harnessing the Radical for Surface Modification of Alginate/Agarose Hydrogel Materials. The validation of the photochemical grafting of polymers on the alginate backbone in the solution phase provides insight into the capability to then surface modify while in the polymer form. As previously mentioned, the moduli of Fe(III) polysaccharide/agarose gels decreased with irradiation with the 405 nm LED due to the breakdown of the carboxylate-containing polysaccharide chain during the photoreaction. However, when Fe(III) AlgG/agarose gels were irradiated with a 405 nm LED (50 mW cm^{-2}) in a 25% MMA solution, there was an increase in the modulus during the first 40 min of irradiation (Figure 4a). This was due to the additional strength gained by the gel

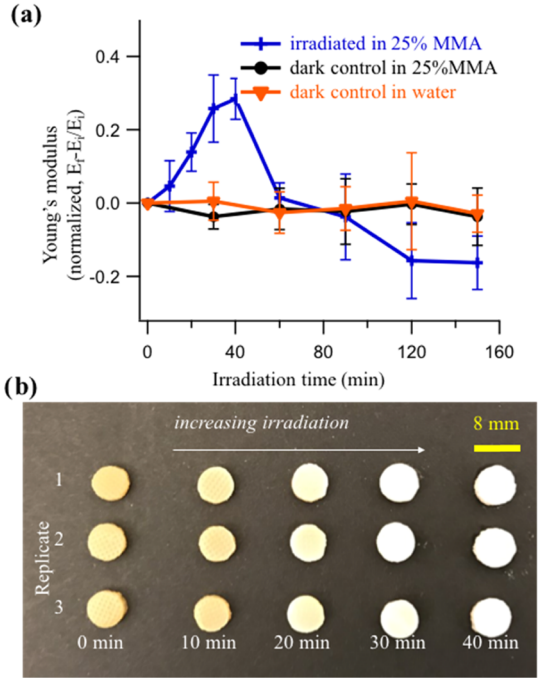

Figure 4. (a) Modulus changes for Fe(III) AlgG/agarose hydrogels with time when stored in dark and irradiated with 405 nm LED (50 mW cm^{-2}) in a 25% MMA solution. (b) Photo of the Fe(III) AlgG/agarose hydrogel surface modified with PMMA for different time intervals (50 mW cm^{-2}, irradiated for 2 h) that were used for the mechanical property testing.

disk from the PMMA coating. After 1 h, a decrease in mechanical properties was observed. This was attributed to polysaccharide chain breakdown and increased porosity due to the Fe(III)−carboxylate photoreaction. Additionally, the white coloration of the gel surface (Figure 4b) increased with the irradiation time and then remained constant after about 30 min, which correlated with the rheology data for increased PMMA formation with time.

Furthermore, contact angle measurements were performed to quantify the hydrophobicity for MMA surface-modified hydrogels. The contact angle of AlgF−agarose at each stage of the surface modification varies drastically (Figure S9). First, in the case of no additive (i.e., AlgF−agarose only), the contact angle is 20.13°, which indicates that the hydrogel surface was hydrophilic. This was attributed to water having strong

https://doi.org/10.1021/acsabm.1c00525
ACS Appl. Bio Mater. 2021, 4, 5765−5775

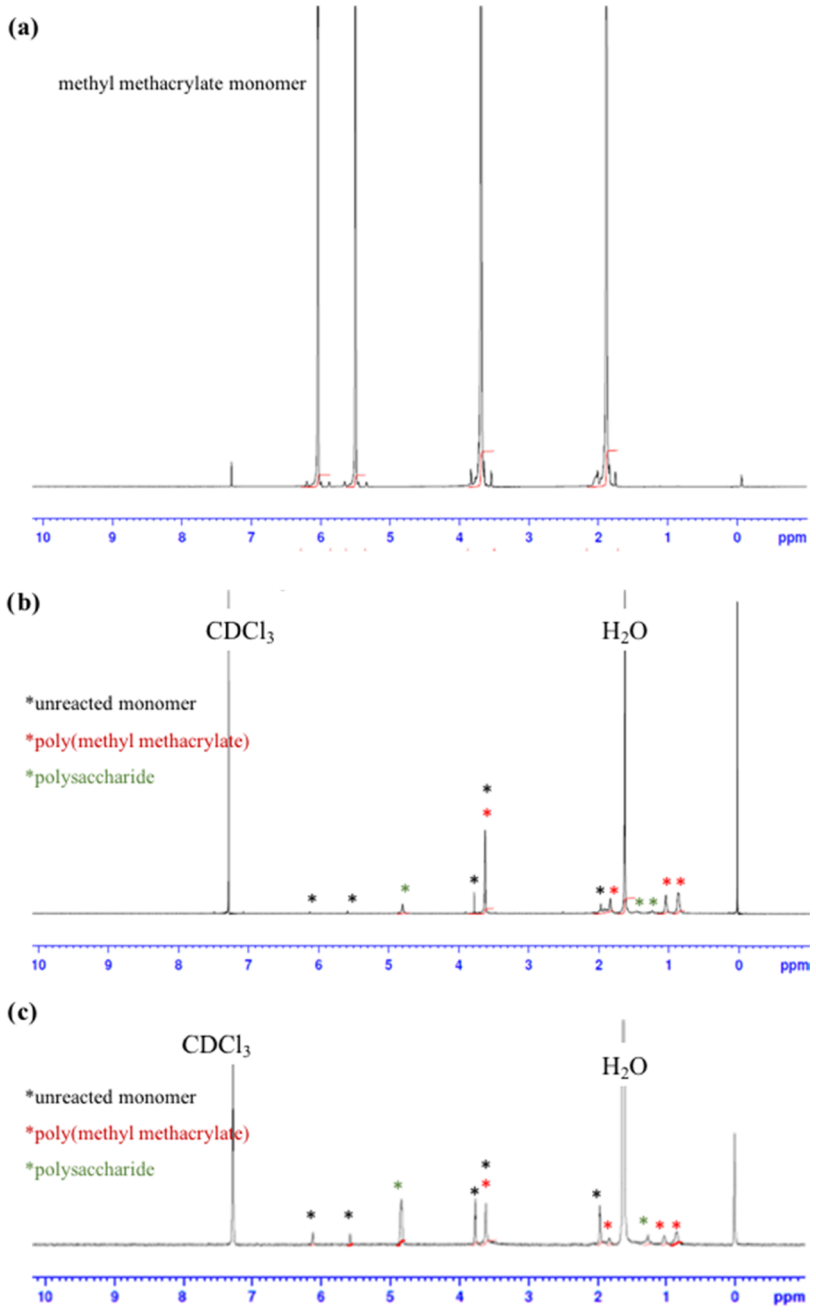

Figure 5. ^{1}H NMR spectrum of (a) methyl methacrylate monomer, (b) poly(methyl methacrylate) polymer on the Fe(III) AlgG/agarose surface, and (c) poly(methyl methacrylate) polymer on the hydrogel interior.

noncovalent interactions with hydrophilic groups (i.e., hydroxyls and carboxylates) within the hydrogel network. Upon addition of Fe(III) into the system, the contact angle increases to 36.59°. This indicates that while the hydrogel is still hydrophilic, the complexation of carboxylates with Fe(III) eliminates the availability of these groups to form strong noncovalent interactions with water. Furthermore, when these Fe(III) hydrogels are irradiated, the contact angle decreases to below that of the AlgF−agarose hydrogel (i.e., 16.95°). As previously discussed, the irradiation of the Fe(III)−carboxylate complex resulted in the decarboxylation of alginate. This process should manifest in a more hydrophobic surface (i.e., higher contact angle) considering the loss of the hydrophilic carboxylates; however, the network structure was altered. With the decarboxylation, the porosity of the hydrogel increased as there were less sites for chain−chain interactions in addition to the loss of Fe(III) complexes. Therefore, this increased porosity resulted in greater instantaneous diffusion into the hydrogel resulting in a lower contact angle. Additionally, with the irradiation of the Fe(III)−AlgF−Agar hydrogel in the presence of MMA, there was a significant increase in the contact angle indicative of the formation of PMMA. This modification altered the surface structure to more hydrophobic groups (i.e., esters), which limited surface interactions with water.

To further validate the composition of the surface layer as PMMA, the white polymeric material formed upon irradiation was analyzed using NMR (Figure 5b,c). More specifically, the ^{1}H NMR of the white surface material was compared to that of the interior hydrogel material (Figure 5c). Both NMR spectra

https://doi.org/10.1021/acsabm.1c00525
ACS Appl. Bio Mater. 2021, 4, 5765−5775

showed that the material was PMMA with the only difference being the material formed inside the hydrogel showed much larger peaks for the polysaccharide compared to the surface material. This was due to the availability of more polysaccharide-based radicals inside the hydrogel so that MMA can polymerize on the radicals generated on the polysaccharide chain and initiate the PMMA polymerization. The surface material was mostly PMMA with a small amount of polysaccharide graft copolymer. The high availability of MMA at the gel−solution interface helped the polymer chain growth.

Gel permeation chromatography (GPC) analysis was performed on the PMMA formed on top of the hydrogels, and it showed two peaks (Figure 6a). The first peak was a

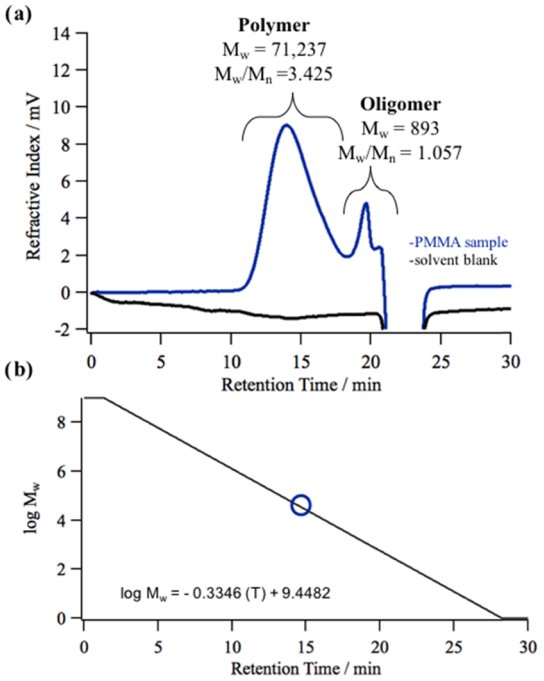

Figure 6. (a) GPC chromatogram of PMMA obtained from the Fe(III) AlgG/agarose gels irradiated in 20% MMA solution for 2.5 h with 405 nm light (50 mW cm^{-2}) (blue) and blank tetrahydrofuran (black). (b) Polystyrene calibration plot used for molecular weight calculations for GPC.

polymer with an average molecular weight of 71 kDa, which accounted for about 90% of the total sample. The degree of polymerization for the PMMA was 710. The second peak was a small oligomer with an average molecular weight of ∼900 Da, which was about 10% of the sample, with a degree of polymerization for the oligomer of 9. This suggested that the PMMA polymerized on the surface of the polymer resulted in a high-molecular-weight copolymer. The oligomer could be attributed to small PMMA chains that were formed by the free carbon dioxide anion radicals and are not attached to polysaccharide chains, instead trapped within the large PMMA polymer layer. Another possibility for the oligomer formation is early termination of the chain growth before they reach high-molecular-weight polymer networks.

Photopolymerization of PANI for Conductive Hydrogels. Further functionalization can be performed on these polysaccharide hydrogels, specifically with conductive polymers, to develop responsive materials. In this study, PANI was postsynthetically polymerized within the hydrogel matrix resulting in a conductive supramolecular network. During the modification process, polysaccharide hydrogels (AlgF/agarose) were coordinated with Fe(III) and then soaked in aniline, which resulted in a characteristic color change from orange to red-brown indicating the integration of aniline (Figure 7a). Upon irradiation of the resultant hydrogel with UV light (405 nm, 50 mW cm^{-2}) in the presence of HCl (dopant), the appearance of a green color was observed which indicates the formation of the emeraldine form of polyaniline (PANI) (Figure 7a). The formation of PANI was further validated through current−voltage (IV) measurements (Figure 7b). As the voltage was applied across the functionalized hydrogel, there was a clear increase in current output compared to that of its nonfunctionalized counterparts indicative of greater conductivity.

The effect of aniline concentration toward the polymerization reaction was also studied under both dark and light conditions in Fe(III) AlgF/agarose gels. In dark conditions, there was an increase in current output as the concentration of aniline increased until it reached a plateau at 20 mM (Figure 8). The initial increase in conductivity was attributed to greater connectivity of PANI chains throughout the network allowing for more efficient electron transfer. At low concentrations, there was not a sufficient amount of monomer to bridge PANI together; therefore, it resulted in oligomers (short, nonproductive polymer chains). Additionally, the plateau at 20 mM indicated that despite greater addition of monomer there was a minimal generation of effective electron pathways. This may be due to an increase in potential termination species and therefore termination occurs more readily, again resulting in nonproductive oligomers.

On the other hand, when performing the reaction with light irradiation (405 nm), there was an initial increase in current output which was then followed by a decrease in current after 20 mM. The initial increase was attributed to greater interconnects of PANI chains, as previously described in the dark conditions, allowing for greater electron transfer. The decrease after 20 mM may be due to "over-polymerization" in which there was a greater number of initiation sites and propagating species which ultimately resulted in oversaturation and greater termination events resulting in shorter PANI chains. The lower current was attributed to a "random walk" in which electrons cannot readily transfer through the network of oligomeric chains, but rather dissipate into the gel.

It must also be noted that the absolute current output was relatively higher and more consistent for PANI hydrogels generated from light-initiated polymerization, with the exception of those produced at the highest aniline monomer concentration (2000 mM). This was a clear indication that there was a change in the polymerization mechanism of PANI between the light and dark conditions. In dark conditions, the initiation of PANI polymerization was achieved through the reduction of Fe(III) to Fe(II), thereby oxidizing aniline to form a radical−cation pair. This reaction was dependent on the kinetics of Fe(III) reduction and the proximity of aniline. In light conditions, however, the initiation was achieved by directly irradiating the Fe(III)−alginate complex, which undergoes ligand-metal charge transfer, ultimately resulting in a radical on the polysaccharide. This radical then initiated the formation of the radical−cation pair on aniline. This light-driven reaction resulted in a more uniform integration of PANI

https://doi.org/10.1021/acsabm.1c00525
ACS Appl. Bio Mater. 2021, 4, 5765−5775

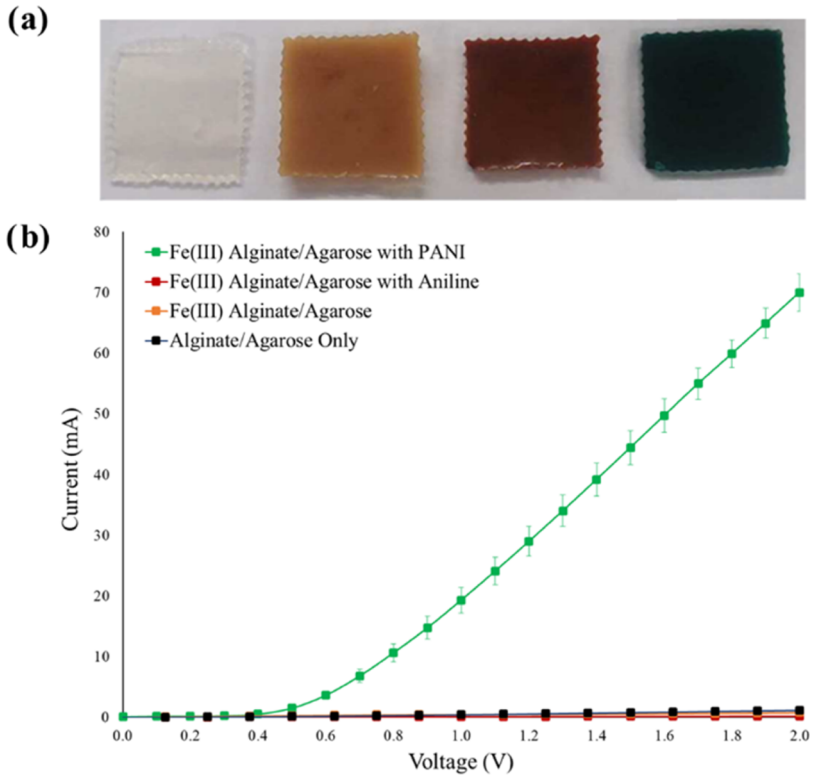

Figure 7. (a) Images of functionalized AlgF−agarose hydrogels at varying stages of PANI synthesis (left to right: no additive, Fe(III), Fe(III) aniline, PANI). (b) *IV* characterization of the corresponding hydrogels at each stage.

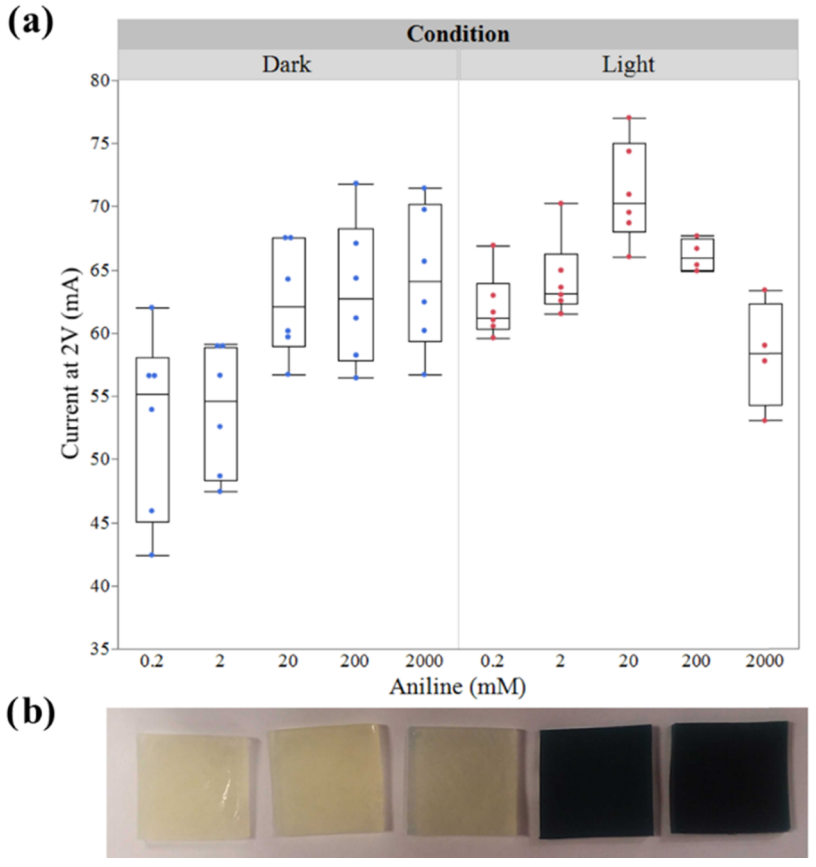

Figure 8. (a) Current output at 2 V for PANI hydrogels as a function of aniline concentration and reaction conditions. (b) Images of PANI Hydrogels as a function of aniline concentration (Left to right increasing concentration).

https://doi.org/10.1021/acsabm.1c00525
ACS Appl. Bio Mater. 2021, 4, 5765−5775

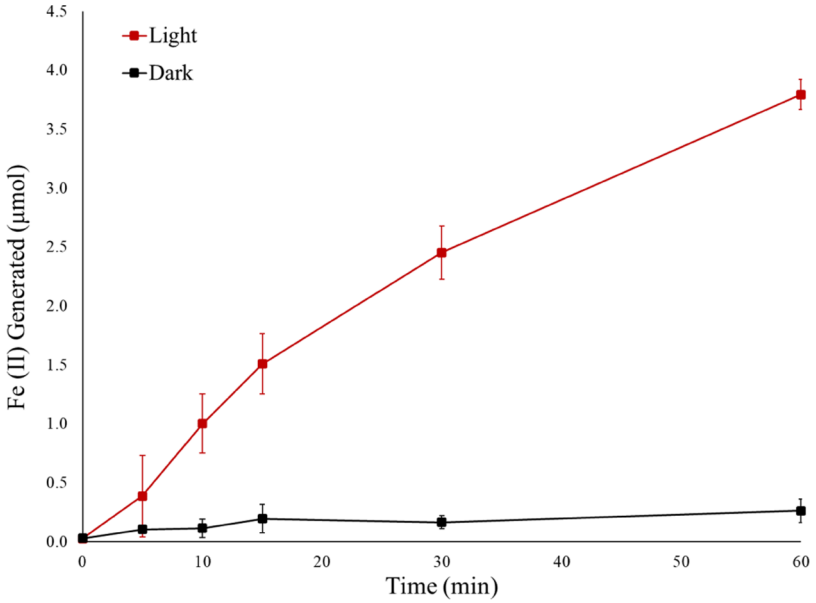

Figure 9. Plot of Fe(II) generation in the presence of a Fe(III)/aniline soaked hydrogel under varying reaction conditions.

as the initiation sites were constrained to the alginate polymer chains.

To further demonstrate the different polymerization mechanisms in each condition, the Fe(II) generation was tracked as a function of time which can be correlated with the rate of radical formation (Figure 9). With irradiation of the Fe(III) AlgF/agarose hydrogel soaked in aniline, there was a clear increase in the generation of Fe(II). This was indicative of an enhanced radical formation on the alginate chain under irradiation with a rate of 0.101 μmol min^{-1} (405 nm, 50 mW cm^{-2}).

On the other hand, in dark conditions, there was a limited increase in the Fe(II) formation which was attributed to a slow rate of Fe(II) generation (0.006 μmol min^{-1}). This again highlights the mechanistic differences in the radical formation between the light-induced reaction and the dark thermal reaction, with an effective order of magnitude of difference in the rates of radical formation. In light conditions, the irradiation of light excited the Fe(III)−Alg complex to allow efficient charge transfer to ultimately form the radical on carboxylic acid and generate Fe(II). In the thermal condition (dark), there was not enough energy to readily charge transfer, resulting in a low generation of Fe(II) as it depended solely on the kinetics of reduction and proximity to aniline.

Additionally, this rate difference in radical generation between the thermal and photoinitiated process was seen in the pectin/agarose hydrogel. Figure 10 shows a photo-patterned material in which light was irradiated on selected areas of the gel thus highlighting the difference between the two initiated mechanisms.

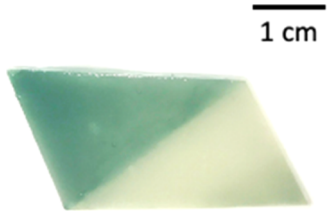

Figure 10. Photo of a Fe(III) pectin/agarose hydrogel soaked in aniline and irradiated in 1 M HCl solution for 30 min with 405 nm (50 mW cm^{-2}) with a photomask.

CONCLUSIONS

Surface modification of hydrogel materials is important to achieve desired physical and chemical properties such as hydrophobicity and conductivity and is extremely important in many applications. This work highlights the importance of inorganic components in natural materials and how Fe(III)−carboxylate photochemistry can be harnessed for modification of natural hydrogel materials. We have shown the Fe(III)−uronic acid photoreaction can be used for photoinitiation of radical polymerization to modify polysaccharide hydrogels. Specifically, we were able to initiate polymerization of acrylic monomers, AAM and MMA, and aniline both in solution and in hydrogel materials. In the case of surface modification with MMA, the hydrogel becomes more hydrophobic and stronger indicating significant changes in the physical properties. On the contrary, with PANI functionalization, there was clear increases in current output indicating the development of electrical properties, albeit at an optimal concentration of monomer. While we present here hydrogel modification with hydrophobic PMMA and conductive PANI, we can envision more advanced experiments such as the patterning of surfaces or even the use of the other radical reactive species to further modify and change the hydrogel chemistry through irradiation. These results are also relevant more broadly to materials science, given the recent reports of tissue engineering using fruit cellulose scaffolds,[25] suggesting different possibilities for using this simple photochemistry to manipulate such natural scaffolds that contain polysaccharides using Fe(III) polyuronic acid photochemistry.

EXPERIMENTAL SECTION

Materials. Low-viscosity sodium alginate from brown algae (AlgM, M_v 45 000 g mol^{-1}) (Lot A112), pectin from citrus peel with 74% galacturonic acid (Lot SLBN9007V M_w 25 000−50 000), ferric chloride hexahydrate (99%), morpholine (99%) acrylamide (AAM), deuterium oxide, aniline (99.5% pure), and deuterated chloroform were all purchased from Sigma-Aldrich and used as received. Only freshly prepared solutions of Fe(III) chloride were

https://doi.org/10.1021/acsabm.1c00525
ACS Appl. Bio Mater. 2021, 4, 5765−5775

used to ensure minimal precipitation of iron oxides/hydroxides. High-guluronate alginate (AlgG), product code IL-6G, was kindly supplied by Kimica Corporation, Japan (M_w 97 000). Congo Red was purchased from Eastman Kodak Company and was certified by the Biological Stain Commission. Soluble potato starch and hydroxylamine hydrochloride were used as received from Mallinckrodt. Agarose was purchased from Life Technologies, Inc. and used as received. Agar powder was purchased from Cynmar Corporation. Methyl methacrylate (MMA) 99% pure was purchased from Alfa Aesar. 1,10 Phenanthroline (99% pure) was used from Aldrich chemical company. Ethanol (200 proof) was purchased from Pharmco-Aaper. Acetone, methanol, and sodium hydroxide (99% pure) were purchased from EMD Millipore corporation. Sodium alginate (AlgF) (Lot #MKCH7131) and hydrochloric acid (ACS reagent, 37%) were purchased from Flinn Scientific.

Methods. *Solution-Phase Radical Polymerization.* A 50 mM solution of sodium alginate (AlgG) was prepared in a 0.9 mM $FeCl_3$ solution. Then, acrylamide (AAM) was added so that the final concentration was 0.42 M. A 0.7 mL aliquot of this solution was pipetted into a quartz cuvette equipped with a septum. The solution was bubbled with nitrogen for at least 5 min before and throughout the reaction. The solution was irradiated with 405 nm light (38 mW cm^{-2}) for different time intervals, and the reaction was quenched by adding a drop of ethanol. The copolymer purification was done by precipitation of the product with acetone first and then extraction with morpholine at 60 °C, and then centrifuged and lyophilized. The quantum yield of polymerization was calculated from the rate of conversion of the monomer, determined from the evolution of the signal at 2.19 ppm in the ^{1}H NMR spectrum, corresponding to the α-proton of the polyacrylamide. To study the effect of the concentrations on the quantum yield, the concentrations of Fe(III) and alginate were kept fixed, and the concentration of AAM was varied from 0.06 to 0.6 M. In a different experiment, the reaction mixture was prepared with the same concentrations of the initiation system, [AAM] = 0.42 M was prepared, and the polymerization quantum yield was measured at different dilutions: 1×, 0.66×, and 0.33×.

Polysaccharide−Agarose Hydrogel Preparation. Hybrid polysaccharide−agarose gels of pectin and alginate were prepared by first adding 200 mg of agarose to 10 mL of water, then 200 mg of polysaccharide was added slowly while on a vortex (the final solution was 2% agarose and 2% polysaccharide by weight). For polysaccharide−agarose gels with Noni and hyaluronic acid, only 100 mg of the polysaccharide (1% by weight) was used along with 200 mg of agarose for gel preparation due to the low solubility of the polysaccharide. The mixture was sonicated for 5 min and then heated in a hot water bath at 96 °C with a stirring rate of 750 rpm for 10 min to ensure everything dissolved. The solution was sonicated for 1 min to remove the air bubbles trapped and then dipped back in the hot water bath for another 2 min without stirring. The solution was poured into a Teflon mold 88.9 mm in diameter with a thickness of 2 mm and covered with a glass plate. The hot solution formed a hydrogel film upon cooling within 10 min. This gel was then soaked in 0.1 M $FeCl_3$ (10 mL) for 2.5 h under dark conditions.

Surface Modification of Hydrogel Samples with Methyl Methacrylate. Polysaccharide−Agarose hydrogels were placed in a Petri dish (h = 1.5 cm, d = 7.5 cm) with 20 mL of acrylic monomer (MMA) solution (25 or 100% by volume) and irradiated for different time intervals with 405 nm light (50 mW cm^{-2}).

Photo Patterning of Hydrogels. Fe(III) pectin/agarose hydrogels were used for photo patterning. The areas of light exposure were controlled using aluminum foil or a wire mesh a photomask. A hydrogel was placed in a Petri dish with a 25% by volume MMA solution and the photomask was placed on top of the hydrogel. Four hundred five nanometer LED (50 mW cm^{-2}) was used for the irradiation for 2 h.

Contact Angle Measurements. The base AlgF−agarose hydrogel was synthesized as previously discussed. For Fe(III) hydrogels, the AlgF−agarose was soaked in 100 mM $FeCl_3$ (10 mL) for 2.5 h in dark and then rinsed with water. The Fe(III) hydrogels with light were soaked in 100 mM $FeCl_3$ (10 mL) for 2.5 h in dark and then irradiated (405 nm) for 1 h while submerged in 10 mL of water. The PMMA hydrogel was synthesized as previously described with 25% MMA. Prior to measuring each hydrogel, the hydrogel was wiped dry to remove any surface water. A 15 μL drop of water was pipetted on the surface of the hydrogel while filming a video (30 fps) using a CASIO Exilim HS EX-ZR700. The video was then uploaded to Tracker, Video Analysis and Modeling Tool software (open source), where the frame in which the drop first settled on the surface was captured. The resultant image was uploaded to ImageJ, Image Processing and Analysis in Java software (open source), to measure the contact angle using the Drop Analysis—LB-ADSA plugin.

Mechanical Property Testing. A TA Instruments Discovery HR-2 rheometer with an 8 mm parallel plate geometry was used for all mechanical property tests. For determining Young's moduli (E') of polysaccharide−agarose hydrogels, dynamic compression experiments were conducted for discs with a diameter of 8 and 2 mm thickness, which were irradiated (405 nm LED, 50 mW cm^{-2}) for various time intervals in water, and Young's moduli were measured at 25 °C. The axial force was 0.5 N, and the samples were compressed up to 5% axial strain with 1 Hz duration for 60 s.

Swelling Experiments. Hydrogels with a thickness of 4 mm were prepared by pouring 20 mL of gel preparation hot solution (2% agarose and 2% pectin) into a Petri dish with a diameter of 7.5 cm. After gelation (10 min after pouring), the hydrogels were soaked in a 0.1 M $FeCl_3$ and stored in dark for 2.5 h. Then, discs with a diameter of 15 mm were punched out from the Fe(III) coordinated hydrogel and irradiated with Thorlabs 405 nm LED light source (50 mW cm^{-2}) for various time intervals (0, 30, 60, 90, 120, and 150 min). These gel disks were then soaked in a 0.025 M ethylenediaminetetraacetic acid (EDTA) solution for 24 h and finally in deionized water for another 30 min. These gel disks were then allowed to air-dry on top of a Teflon surface for 24 h. Air-dried gel disks were weighed and placed in vials separately with 20 mL of deionized water and allowed to swell for 20 h at 25 °C. Fully swollen gel disks were carefully wiped with a Kimwipe and weighed again. The swelling ratio of each gel was calculated using eq 10.

$$\text{swelling ratio} = \frac{\text{weight of fully swollen}}{\text{weight of dry gel}} \tag{10}$$

Scanning Electron Microscopy (SEM). Hydrogels, surface modification with MMA, were frozen with liquid nitrogen and lyophilized using a LABCONCO Freeze Dry System Free zone 4.5 under dark conditions. Then, the sample was sputter-coated with Au/Pd using a Hummer VI-A sputter coater machine. SEM images were collected on a Hitachi S-2700 scanning electron microscope at 10 kV.

Light Microscopy. Hydrogel samples photopatterned were observed and imaged using an OMAX microscope equipped with a A3514U3 digital camera with a magnification of 10×. Surface-modified hydrogel sample cross sections were observed and imaged using a Zeiss Stemi 2000-C optical microscope with the use of bottom light set at bright (BF+) mode.

Contact Angle Measurements. The water contact angles on surface-modified hydrogel discs were determined using a Tantec Model CAM-MICRO Contact Angle Meter. Hydrogel discs which were stored in water to avoid drying were gently tapped with a Kimwipe to remove the surface water. Then, the water contact angle was measured as soon as the water droplet was placed on the hydrogel surface. Three gels were used for each type of hydrogels, and average and standard deviation were calculated.

Gel Permeation Chromatography. Replications of 3 mg each of dry PMMA that was formed on top of the hydrogels were dissolved in 3 mL of tetrahydrofuran, and the molecular weight distribution was determined using an Ecosec HLC-83280 GPC with RI detector. Molecular weight was determined by comparison to a calibration curve of PStQuick C (MW 2 110 000−500) and PStQuick D (MW 1 090 000−2420) polystyrene standards.

^{1}H NMR. PMMA formed on the gel surface was dissolved in deuterated chloroform, and proton NMR was recorded on a Bruker

https://doi.org/10.1021/acsabm.1c00525
ACS Appl. Bio Mater. 2021, 4, 5765−5775

AVANCE III spectrometer operating at 500 MHz. For the material formed inside the gel, the hydrogel disks were sliced and PMMA was dissolved in deuterated chloroform for NMR analysis.

Surface Modification of Hydrogel with Polyaniline (PANI). AlgF/agarose gels were prepared in a 43 mm x 43 mm silicone mold as previously described. The resultant gel was then soaked in a 0.1 M $FeCl_3$ (10 mL) for 2.5 h under dark conditions. After soaking, the gel was rinsed with DI water and soaked in aniline (10 mL) for an hour in dark conditions. This gel was then rinsed with DI water and soaked in 1 M HCl (10 mL) under UV irradiation (405 nm, 50 mW cm^{-2}). The resultant PANI-AlgF/agar gel was rinsed with DI water.

I–V Characterization of Hydrogels. The current output of the hydrogels was measured as a function of voltage using a Keithley 2450 Sourcemeter (Tektronix). During measurement, the probes (20 mm apart) were inserted through the depth of the gel. The voltage was increased to 2 in 0.1 V steps.

■ ASSOCIATED CONTENT

Supporting Information

The Supporting Information is available free of charge at https://pubs.acs.org/doi/10.1021/acsabm.1c00525.

Photopolymerization of AAM and MMA, circular dichroism spectra for alginate, change of hydrodynamic radius with irradiation time, mechanical property changes of Fe(III)−AlgG−agarose gels with time, photos of gels with Congo Red dye on them before and after irradiation, photos of irradiation of gels in a nitrogen environment, GPC spectrum for PMMA, and contact angles for different Fe(III)−polysaccharide−agarose gels (PDF)

Electronic supporting information containing a video highlighting changes in hydrophobicity in the gels is also available (MP4)

■ AUTHOR INFORMATION

Corresponding Authors

Jason J. Keleher − *Department of Chemistry, Lewis University, Romeoville, Illinois 60446, United States;* orcid.org/0000-0003-4310-6094; Email: keleheja@lewisu.edu

Alexis D. Ostrowski − *Department of Chemistry and Center for Photochemical Sciences, Bowling Green State University, Bowling Green, Ohio 43403, United States;* orcid.org/0000-0002-3207-1845; Email: alexiso@bgsu.edu

Authors

M. H. Jayan S. Karunarathna − *Department of Chemistry and Center for Photochemical Sciences, Bowling Green State University, Bowling Green, Ohio 43403, United States;* orcid.org/0000-0002-2805-0806

Abigail N. Linhart − *Department of Chemistry, Lewis University, Romeoville, Illinois 60446, United States;* orcid.org/0000-0002-6540-8248

Giuseppe E. Giammanco − *Department of Chemistry and Center for Photochemical Sciences, Bowling Green State University, Bowling Green, Ohio 43403, United States;* orcid.org/0000-0001-8553-4607

Amie E. Norton − *Department of Chemistry and Center for Photochemical Sciences, Bowling Green State University, Bowling Green, Ohio 43403, United States*

Jackson J. Chory − *Department of Chemistry and Center for Photochemical Sciences, Bowling Green State University, Bowling Green, Ohio 43403, United States*

Complete contact information is available at: https://pubs.acs.org/10.1021/acsabm.1c00525

Author Contributions

The manuscript was written through the contributions of all authors. All authors have given approval to the final version of the manuscript.

Notes

The authors declare no competing financial interest.

■ ACKNOWLEDGMENTS

This work was partially supported by Bowling Green State University through start-up funds. This work was partially supported by an NSF CAREER award, Division of Chemistry, Chemical Structure, Dynamics and Mechanisms-B Program and Division of Materials Research Polymers program (CHE-1653892) to A.D.O. Support was provided to M.H.J.S.K. by the Herman Frasch Foundation for Chemical Research (811-17F). The authors thank Prof. Sivaguru Jayaraman and Ravi Singathi at BGSU Department of Chemistry for their help with GPC. The authors also thank Dr. Marilyn Cayer at the Bowling Green State University Department of Life Sciences SEM Center. Additional support was received from the Colonel S. and Lyla Doherty Center for Aviation and Health Research at Lewis University to J.J.K.

■ ABBREVIATIONS USED

AAM, acrylamide; MMA, methyl methacrylate; PMMA, poly(methyl methacrylate); PANI, polyaniline; AlgG, sodium alginate G (35% mannuronate); AlgM, sodium alginate M (61% mannuronate); AlgF, sodium alginate from Flinn Scientific; M_w, molecular weight; CD, circular dichroism; LED, light-emitting diode; NMR, nuclear magnetic resonance; SEM, scanning electron microscope; GPC, gel permeation chromatography; EDTA, ethylenediaminetetraacetic acid; AFM, atomic force microscopy

■ REFERENCES

(1) Kabiri, K.; Omidian, H.; Zohuriaan-Mehr, M. J.; Doroudiani, S. Superabsorbent Hydrogel Composites and Nanocomposites: A Review. *Polym. Compos.* **2011**, *32*, 277−289.

(2) Bains, D.; Singh, G.; Kaur, N.; Singh, N. Development of Biological Self-Cleaning Wound-Dressing Gauze for the Treatment of Bacterial Infection. *ACS Sustainable Chem. Eng.* **2019**, *7*, 969−978.

(3) Wang, K.; Hou, D.; Wang, J.; Wang, Z.; Tian, B.; Liang, P. Hydrophilic Surface Coating on Hydrophobic PTFE Membrane for Robust Anti-Oil-Fouling Membrane Distillation. *Appl. Surf. Sci.* **2018**, *450*, 57−65.

(4) Xu, G.; Liu, P.; Pranantyo, D.; Neoh, K.-G.; Kang, E.-T.; Lay-Ming Teo, S. One-Step Anchoring of Tannic Acid-Scaffolded Bifunctional Coatings of Antifouling and Antimicrobial Polymer Brushes. *ACS Sustainable Chem. Eng.* **2019**, *7*, 1786−1795.

(5) Han, L.; Liu, K.; Wang, M.; Wang, K.; Fang, L.; Chen, H.; Zhou, J.; Lu, X. Mussel-Inspired Adhesive and Conductive Hydrogel with Long-Lasting Moisture and Extreme Temperature Tolerance. *Adv. Funct. Mater.* **2018**, *28*, No. 1704195.

(6) Dispenza, C.; Presti, C. L.; Belfiore, C.; Spadaro, G.; Piazza, S. Electrically Conductive Hydrogel Composites Made of Polyaniline Nanoparticles and Poly(N-Vinyl-2-Pyrrolidone). *Polymer* **2006**, *47*, 961−971.

(7) Guo, B.; Finne-Wistrand, A.; Albertsson, A.-C. Facile Synthesis of Degradable and Electrically Conductive Polysaccharide Hydrogels. *Biomacromolecules* **2011**, *12*, 2601−2609.

(8) Wu, Y.; Chen, Y. X.; Yan, J.; Yang, S.; Dong, P.; Soman, P. Fabrication of Conductive Polyaniline Hydrogel Using Porogen Leaching and Projection Microstereolithography. *J. Mater. Chem. B* **2015**, *3*, 5352−5360.

(9) Taşdelen, B. Conducting Hydrogels Based on Semi-Interpenetrating Networks of Polyaniline in Poly(Acrylamide-Co-Itaconic Acid) Matrix: Synthesis and Characterization. *Polym. Adv. Technol.* **2017**, *28*, 1865−1871.
(10) Zhu, F.; Lin, J.; Wu, Z. L.; Qu, S.; Yin, J.; Qian, J.; Zheng, Q. Tough and Conductive Hybrid Hydrogels Enabling Facile Patterning. *ACS Appl. Mater. Interfaces* **2018**, *10*, 13685−13692.
(11) Pyarasani, R. D.; Jayaramudu, T.; John, A. Polyaniline-Based Conducting Hydrogels. *J. Mater. Sci.* **2019**, *54*, 974−996.
(12) Corrigan, N.; Yeow, J.; Judzewitsch, P.; Xu, J.; Boyer, C. Seeing the Light: Advancing Materials Chemistry through Photopolymerization. *Angew. Chem., Int. Ed.* **2019**, *58*, 5170−5189.
(13) Neumann, M. G.; Schmitt, C. C.; Rigoli, I. C. The Photoinitiation of MMA Polymerization in the Presence of Iron Complexes. *J. Photochem. Photobiol., A* **2003**, *159*, 145−150.
(14) Zhang, J.; Campolo, D.; Dumur, F.; Xiao, P.; Fouassier, J. P.; Gigmes, D.; Lalevée, J. Iron Complexes as Photoinitiators for Radical and Cationic Polymerization through Photoredox Catalysis Processes. *J. Polym. Sci., Part A: Polym. Chem.* **2015**, *53*, 42−49.
(15) Telitel, S.; Dumur, F.; Campolo, D.; Poly, J.; Gigmes, D.; Pierre Fouassier, J.; Lalevée, J. Iron Complexes as Potential Photocatalysts for Controlled Radical Photopolymerizations: A Tool for Modifications and Patterning of Surfaces. *J. Polym. Sci., Part A: Polym. Chem.* **2016**, *54*, 702−713.
(16) Faust, B. C.; Zepp, R. G. Photochemistry of Aqueous Iron(III)-Polycarboxylate Complexes: Roles in the Chemistry of Atmospheric and Surface Waters. *Environ. Sci. Technol.* **1993**, *27*, 2517−2522.
(17) Barbeau, K.; Rue, E. L.; Bruland, K. W.; Butler, A. Photochemical Cycling of Iron in the Surface Ocean Mediated by Microbial Iron(Iii)-Binding Ligands. *Nature* **2001**, *413*, 409−413.
(18) Lueder, U.; Jørgensen, B. B.; Kappler, A.; Schmidt, C. Photochemistry of Iron in Aquatic Environments. *Environ. Sci.: Processes Impacts* **2020**, *22*, 12−24.
(19) Giammanco, G. E.; Sosnofsky, C. T.; Ostrowski, A. D. Light-Responsive Iron(III)-Polysaccharide Coordination Hydrogels for Controlled Delivery. *ACS Appl. Mater. Interfaces* **2015**, *7*, 3068−3076.
(20) Karunarathna, M. H. J. S.; Ayodele, M. J.; Giammanco, G. E.; Brugh, A. M.; Muizzi, D. A.; Bauman, M. A.; Torelli, A. T.; Alabanza, A. M.; Forbes, M. D. E.; Ostrowski, A. D. Fe(III)-Polyuronic Acid Photochemistry: Radical Chemistry in Natural Polysaccharide. *Photochem. Photobiol. Sci.* **2021**, *20*, 255−263.
(21) Giammanco, G. E.; Ostrowski, A. D. Photopatterning the Mechanical Properties of Polysaccharide-Containing Gels Using Fe3+coordination. *Chem. Mater.* **2015**, *14*, 4922−4925.
(22) Yeow, J.; Chapman, R.; Gormley, A. J.; Boyer, C. Up in the Air: Oxygen Tolerance in Controlled/Living Radical Polymerisation. *Chem. Soc. Rev.* **2018**, *47*, 4357−4387.
(23) Kuhn, H. J.; Braslavsky, S. E.; Schmidt, R. Chemical Actinometry. *Pure Appl. Chem.* **1989**, *61*, 187−210.
(24) Odian, G. *Principles of Polymerization*; 4th ed.; Wiley, 2004.
(25) Modulevsky, D. J.; Lefebvre, C.; Haase, K.; Al-Rekabi, Z.; Pelling, A. E. Apple Derived Cellulose Scaffolds for 3D Mammalian Cell Culture. *PLoS One* **2014**, *9*, No. e97835.

https://doi.org/10.1021/acsabm.1c00525
ACS Appl. Bio Mater. 2021, 4, 5765−5775